XANES measurements showed that the local structure surrounding Fe and Ti ions was similar. Dielectric study showed that the samples underwent a typical relaxor ferroelectric behavior while the magnetic properties showed very interesting behavior with square saturated magnetic hysteresis loops.

Keywords: Dielectric · Lead iron tantalite · Lead zirconate titanate · Magnetic properties · Multiferroic

#### 1. Introduction

The combination of ferroelectric and ferromagnetic properties in one material is very attractive for many potential applications, such as actuators, sensors, modulators, transducers and memories. The development of materials based on perovskite structure seems to be the most popular and effective way to obtain multiferroic materials. Because the choice of only single-phase materials exhibiting coexistence of ferroelectricity and ferromagnetism is limited, several multiferroic compounds with separate or combined ferroelectric and ferromagnetic properties have been reported, such as (Bi<sub>1-x</sub>La<sub>x</sub>)FeO<sub>3</sub>-PbTiO<sub>3</sub> [1], Pb(Fe<sub>0.33</sub>W<sub>0.67</sub>)O<sub>3</sub>-PbTiO<sub>3</sub> [2], Pb(Fe<sub>0.5</sub>Nb<sub>0.5</sub>)O<sub>3</sub>-Pb(Zr<sub>0.2</sub>Ti<sub>0.8</sub>)O<sub>3</sub> [3], Pb(Fe<sub>2/3</sub>W<sub>1/3</sub>)O<sub>3</sub>-BiFeO<sub>3</sub> [4], Pb(Zr<sub>0.52</sub>Ti<sub>0.48</sub>)O<sub>3</sub>-BiFeO<sub>3</sub> [5], xNiFe<sub>2</sub>O<sub>4</sub>-Ba<sub>0.8</sub>Sr<sub>0.2</sub>TiO<sub>3</sub> [6] and CoFe<sub>2</sub>O<sub>4</sub>-Nb-Pb(Zr,Ti)O<sub>3</sub> [7]. A review of the literature indicates that Pb-based perovskites with the general formula Pb(B'B'')O<sub>3</sub> are of special interest. Because of the intense interest in these multiferroic materials with potential electronic applications, investigation of their dielectric and structural data is very important. Although many published reports have been devoted to various relaxors, only a limited amount of data concerning (1-x)PFT-xPZT [8] can be found in the literature.

Pb(Fe<sub>0.5</sub>Ta<sub>0.5</sub>)O<sub>3</sub>, or PFT, is a perovskite relaxor, being a single-phase multiferroic with diffuse ferroelectric transition at about -30 °C and two antiferromagnetic transitions, one of which has been reported in the range from -93 to -140 °C [9,10] and the other at -264 °C [11], in which magnetic Fe<sup>3+</sup> (3 $d^5$ ) and nonmagnetic Ta<sup>5+</sup> (5 $d^0$ ) share the B-site of the perovskite structure. This compound shows simultaneous magnetic and electric ordering in the same phase. PFT belongs to a group of relaxors that are difficult to synthesize. However, relatively low sintering temperature ( $\sim 1,050$  °C), high dielectric permittivity and high resistivity make PFT a promising material for capacitors.

On the other hand,  $Pb(Zr_{1-x}Ti_x)O_3$ , or PZT, is one of the most well-known, efficient and widely applied ferroelectric materials. It has a perovskite structure with  $Ti^{4+}$  and  $Zr^{4+}$  ions occupying the A-site at random [12,13]. The morphotropic phase boundary (MPB) [14] is an essential parameter to be considered; in this region, tetragonal and rhombohedral phases coexist and consequently the properties of these materials are improved. At room temperature, the boundary is at the point Zr/Ti = 53/47. Moreover, PZT exhibits a high electromechanical coupling coefficient, high  $T_c$  values, can be easily poled and possesses a wide range of dielectric permittivity.

A detailed literature survey shows that there has been only one study on the structural phase transition and multiferroic properties of  $(1-x)Pb(Zr_{0.53}Ti_{0.47})O_3$ - $xPb(Fe_{0.5}Ta_{0.5})O_3$  ceramics with x = 0.3 and 0.4. Sanchez *et al.* [8] reported on the temperature dependent X-ray scattering, Raman, dielectric, magnetization and polarization of these ceramics. However, so far no one has studied the other compositions of this system: i.e.  $(1-x)Pb(Fe_{0.5}Ta_{0.5})O_3$ - $xPb(Zr_{0.53}Ti_{0.47})O_3$  with x = 0.1-0.5. Thus, this work aimed to fabricate of multiferroics based on PFT relaxors and PZT ferroelectrics in the form of bulk ceramics and to study phase

formation, the structural, dielectric and magnetic properties of  $(1-x)Pb(Fe_{0.5}Ta_{0.5})O_3-xPb(Zr_{0.53}Ti_{0.47})O_3$  with x = 0.1-0.5 multiferroic ceramics.

#### 2. Experimental procedures

Synthesis of PFT and PZT was performed by a conventional solid-state reaction. A two-step wolframite method developed for relaxors by Swartz et al. [15] was used to synthesize PFT. First, finely mixed powders of Fe<sub>2</sub>O<sub>3</sub> and Ta<sub>2</sub>O<sub>5</sub> were calcined at 1,000 °C for 4 h in an alumina crucible after being ball-milled in ethanol for 24 h and dried at 120 °C. The reaction product FeTaO<sub>4</sub> was then ground and mixed with PbO for 24 h via ball-milling technique. The mixed powders were calcined at 850 °C for 2 h. PZT was synthesized by modified mixed-oxide method with two mixed oxide reaction stages: in the first stage, PbO was reacted with ZrO2 to give PbZrO3 (PZ); and in the second stage, TiO2 was reacted with PZ to give the final product of perovskite PZT. Conditions for optimizing the calcination of PZ and PZT powders were at temperatures of 800 and 900 °C, respectively. This simple procedure was used to prepare PFT-PZT samples. Different amounts (0.1-0.5) of PZT powders were ultrasonically dispersed in ethanol for 10 min before ball-milling with PFT powders for 2 h. The slurries were at 120 °C. The powder mixtures were formed into pellets by adding 3 wt% polyvinyl alcohol binder, prior to pressing in a uniaxial press at 100 MPa. Sintering of two-phase samples was performed at 1,200 °C for 2 h in a closed alumina crucible. These temperatures are high enough to obtain the single phase of PFT-PZT without calcinating. A PbO atmosphere was also maintained during sintering, using PZ powders in order to minimize the lead loss due to evaporation [16].

4

For structural studies, the samples were characterized by XRD using Cu  $K_{\alpha}$  radiation in a  $2\theta$  range from  $20^{\circ}$ – $80^{\circ}$  with a scan rate of 0.02 °/min. The local structure around Fe and Ti ions of the samples was obtained by synchrotron X-ray Absorption Near Edge Structure (XANES) technique in fluorescence mode at the Synchrotron Light Research Institute, Nakhon Ratchasima, Thailand, using a SUT-NANOTEC-SLRI beamline (BL-5). The bulk density was determined by using the Archimedes principle in distilled water and the relative density calculated using the theoretical density of PFT. Fracture surface of the samples was examined with a scanning electron microscopy (SEM: JEOLJSM-840A). To measure the dielectric properties, gold electrodes were formed on both parallel surfaces of the sintered disks. The dielectric properties were determined as a function of temperature (from 25–200 °C) and frequency (from 1–1000 kHz) using a LCR meter. Magnetization measurements were carried out at room temperature by a vibrating sample magnetometer (VSM) in a magnetic field up to 8 kOe.

#### 3. Results and discussion

XRD analysis of the sintered samples revealed a two-phase composition. The strongest peaks in the pattern could be attributed to the PFT and PZT phases. The individual PFT (Joint Committee on Powder Diffraction Standard [JCPDS] card no. 15-416) and PZT (JCPDS card no. 01-70-4264) phases stabilized in cubic and tetragonal structures, respectively. All the reflection peaks were indexed using the observed interplanar spacing (d). These values suggested that there was a change in the crystal structure from cubic to mixed-cubic/tetragonal. As shown in Fig. 1, all diffraction peaks of samples with x = 0.1–0.5 shifted toward lower angles. Moreover, it is especially evident that the sharp (200), (211) and (220) peaks became broader. This may be due to the fact that Fe<sup>3+</sup> ions were substituted by Ti<sup>4+</sup>

ions; the Ti<sup>4+</sup> ionic radius (61 pm) is slightly larger than that of the Fe<sup>3+</sup> ion (55 pm), resulting in an increase in unit cell volume [17]. The replacement of Fe<sup>3+</sup> ions by Ti<sup>4+</sup> ions could be confirmed by XANES technique. Careful observation also indicated that a very small amount of pyrochlore phase (marked with \* on the XRD pattern) was detected in the PFT sample after sintering at 1200 °C and was also found in the PFT-PZT samples. This indicated that the pyrochlore phase formed during PFT synthesis. The exact composition of the pyrochlore phase in these samples is not known. While almost all the pyrochlore phases are diamagnetic or paramagnetic, the pyrochlore phase to some extent has a certain effect on magnetization, depending on the strength of the diamagnetic (or paramagnetic) signal.

The Fe and Ti K-edge XANES spectra of PFT-PZT samples with x = 0.1, 0.3 and 0.5 are shown in Figs. 2–4; these are also compared with the spectra of Fe-metal, FeO (Fe<sup>2+</sup>), Fe<sub>2</sub>O<sub>3</sub> (Fe<sup>3+</sup>) and Fe<sub>3</sub>O<sub>4</sub> (mixed Fe<sup>2+</sup> and Fe<sup>3+</sup>) standards for Fe K-edge and PZT single crystal for Ti K-edge, respectively. The high local sensitively of XANES technique allows better structural characterization of the supported phases and confirms the XRD results. In Fig. 2, the normalized data were analyzed in the XANES region between 7100 and 7210 eV. The excited energy (E<sub>0</sub>) for x = 0.1, 0.3 and 0.5 was 7133 eV, close to the E<sub>0</sub> of the Fe<sub>2</sub>O<sub>3</sub> standard. It can be identified that the oxidation state of Fe ions in all PFT-PZT samples is equal to +3. The Fe K-edge XANES spectra of these samples also reveal that the spectral features are not significantly changed with the compositions of the PFT compound (Fig. 3). Small changes in the spectra were caused by the variation in the lattice parameters with changing compositions. Moreover, all the spectral features are very similar to those of Ti K-edge of PZT single crystal. This result suggested that the Fe ions were located at the same site as Ti ions. Fig. 4 shows that the features of Ti K-edge XANES spectra of all samples are very similar to those of Fe K-edge XANES spectra, demonstrating that the local structure of Fe

and Ti ions are similar. Therefore, it could be concluded that the Fe ions are replaced by Ti ions, and vice versa. More importantly, the XANES results also indicated that there was no trace of Fe compounds detected in the prepared samples.

The influence of PZT additions on the relative density of PFT samples is shown in Table 1. Generally, it is evident that PFT-PZT could be sintered to above 90% of the theoretical density even at a temperature as low as 1200 °C. As the PZT content increases from 0.1 to 0.3, the relative density of the samples increases and reaches the maximum value 96% of the theoretical density at x = 0.3 and then slightly decreases with increasing the PZT with x = 0.4. The result indicated that the introduction of PZT additive into PFT composition promoted the densification in the low sintering temperature. Fig. 5 shows SEM micrographs for the fracture surface of PFT-PZT ceramics with x = 0.1-0.5 and grain sizes are also shown in Table 1. As shown in micrographs, the solid solution ceramic systems exhibited a fine grain structure. It is clear that a uniform and homogeneous microstructure with fewer pores is obtained from the ceramics with x = 0.3 and 0.4. Moreover, micrographs show homogeneity with well-grown grains and possess equiaxed grains with good grain-packing. On the other hand, the samples with x = 0.1 and 0.2 - Fig. 5 (a) and (b) – show abnormal grain growth. These are important quantitative aspects of liquid phase formed by the reaction between PbO and Fe<sub>2</sub>O<sub>3</sub> at grain boundaries and increases the diffusion path length and then path of the liquid phase is volatilized, giving rise to the pore inside the ceramics.

The PFT-PZT samples exhibited broad maxima in dielectric constant versus temperature plots, as well as a strong dependency of permittivity on frequency. Fig. 6(a) showed the temperature dependence of dielectric constant of PFT at various frequencies. It can not be observed the maximum dielectric and  $T_c$  because the diffuse ferroelectric transition at about -30 °C. In Figs. 6(b) and (c), the dielectric constants ( $\varepsilon_i$ ) for 0.7PFT-0.3PZT and

7

0.6PFT-0.4PZT are shown as a function of temperature at frequencies of 1-1000 kHz. Here, the dielectric constant increases gradually with an increase in temperature up to the transition temperature  $(T_c)$  and then decreases. The region around the dielectric peak was apparently broadening. The broadening of the peak occurs mainly due to compositional fluctuation and/or substitution disordering in the arrangement of cations in one or more crystallographic sites of the PFT-PZT structure. Phase transitions for both compositions are of typical second order ferroelectric phase transitions, in agreement with the findings of Sanchez et al. [8]. Moreover, it can be noticed that there is the board hump in dielectric constant for both of samples. The board hump characteristic in dielectric constant obtained with precalcined compounds are most easily explained as due to the failure of ions to interdiffuse fully during the subsequent sintering to form a homogeneous composition. The resulting inhomogeneity comprises regions with different Curie points and the net effect is the board hump in dielectric constant. For instance, (Ba<sub>1-x</sub>Sr<sub>x</sub>)TiO<sub>3</sub> compositions with different x, calcined separately with the same method used in this work, yield a single peak corresponding to their average composition when sintered to full density in air because of the relatively rapid interdiffusion of Ba2+ and Sr2+ ions. In this work, highly charged ions such as Zr4+ diffuse more slowly and can give rise to inhomogeneous composition [18, 19]. The  $T_c$  for x = 0.3 and 0.4 were determined to be 95 °C and 145 °C at 1 kHz, respectively, indicating an upward shift with increased PZT content. Broadening of dielectric constant curves has also been previously reported, e.g. for PZTFT [8] and for PFT doped with 0.3 mol% La<sub>2</sub>O<sub>3</sub> [20]. The maxima of dielectric constants corresponded to the diffuse ferroelectric-paraelectric transition. High and broad maxima at levels of 5000-96000 and 9600-77000 for 0.7PFT-0.3PZT and 0.6PFT-0.4PZT samples were observed, which decreased with increasing frequency. Compared with PZT-based ceramics, these values were higher than those determined by Nomura et al. [21] and Zhu et al. [22]. The enlargement of maximum

dielectric constant values when adding PZT could be explained by the incorporation of additional amounts of  $Ti^{4+}$  in the B-site of the perovskite structure, which could enhance the chemical microinhomogenity of the relaxor, thus entailing an increase in a values [20,23], as indicated by XANES results. The value of the dielectric constant of 0.7PFT-0.3PZT was higher than that of the 0.6PFT-0.4PZT sample; this could be explained by the fact that it has a high number of ferrous ions whose exchange  $Fe^{2+} \leftrightarrow Fe^{3+}$  gives rise to high dielectric polarization. The electron exchange between  $Fe^{2+}$  and  $Fe^{3+}$  ions on the octahedral site of PFT is thermally activated by increasing temperature. This electron exchange causes local displacement in the dielectric of the external applied electric field and dielectric polarization in the ferromagnetic materials [24].

More interestingly, beside the slight change in the density and microstructure between 0.7PFT-0.3PZT and 0.6PFT-0.4PZT samples, it can be seen that all plots show the similar tendency of variation. The higher dielectric constants are obtained for 0.7PFT-0.3PZT because the samples have higher density with fewer pores, which lead to decrease of the energy loss and improvement of the dielectric properties. Moreover, with decreasing grain size, a decrease of dielectric constant is observed. Thus the grain size seems to play an important role in increasing the maximum dielectric constant. There are many factors for grain size effects in dielectric properties. The model mainly includes intrinsic and extrinsic effect [25]. The intrinsic effect is mainly the consequence of surface effect, which denotes a composite structure of the grains and this also supports the board hump behavior in dielectric constant. As known, grain boundaries are nonferroelectric phase without spontaneous polarization ( $P_s$ ) because grain boundaries include lots of impurities and defects and these impurities can diffuse into grains, the  $P_s$  is suppressed. This will make the grain inhomogeneous, in the same results with other works [26-28]. Another factor is extrinsic

effect. This point has been discussed in detailed by Zhao [25]. The volume fraction of grain boundary increases with the decrease of grain size. This consequently led to lower dielectric constant of 0.6PFT-0.4PZT.

Moreover, from Fig. 6, it can be seen that there is a larger difference between the maximum dielectric constant at 1 kHz and other frequencies. Many factors could be attributed to this observation, one of which is the electric conductivity. The DC resistance of these ceramics is very large (in order to  $10^4~\Omega$ ), which could be determined by that of interelectrode surfaces. However, at 1 kHz, the DC resistance of the ceramics is lower than other frequencies. This could be caused by electric charge from silver electrode. Other factors could be the polarizability of these ceramics. The various polarization processes are important. Dielectric constant arises from electrons, ions, dipoles, defects and space charge. At low enough frequencies (for instance 1 kHz), the value of dielectric constant measured could be identical to the static value and all polarizability terms contributed to dielectric constant, while at higher frequencies this contribution are lost [19].

PFT-PZT samples showed well-behaved magnetization (M) versus applied field (H) hysteresis at room temperature, as shown in Fig. 7. All samples showed square saturated magnetization loops. These systems showed low remanent magnetization at room temperature, which was comparable to the known room-temperature multiferroics including BiFeO<sub>3</sub> and the other lead-based multiferroic relaxors [29–31]. However, the magnetization values of all PFT-PZT samples were similar to those of BF-BMT-PT systems [32]. These low remanent magnetization values could be explained by the Fe magnetic moments in PFT-PZT as coupled ferromagnetically within the pseudo-cubic (111) plane and antiferromagnetically between the adjacent planes. There is a spiral spin structure from superimposed antiferromagnetic ordering which leads to cancellation of macroscopic

magnetization. Moreover, Ti ion substitution could result in the occurrence of antiferroic phases of ordered double perovskite  $A_2B'B''O_6$  with one magnetic and one nonmagnetic B cation [33, 34]. The influence of B-site cation distribution on the magnetic properties of PFT was studied by first-principle calculations performed on differently ordered supercells of the long-range disordered Pm $\overline{3}$ m phases [10, 35]. Another reason was described by Sanchez et al. [8]. In their work, field-cooled (FC) and zero-field-cooled (ZFC) studies were carried out over a wide temperature range. Neel temperature related to the original PFT was not observed, suggesting the existence of super-antiferromagnetic and/or super-paramagnetic clusters far above the ambient temperature [29, 36]. These models are used to explain the possible presence of weak magnetism in lead-based multiferroics. The explanation of the observed weak magnetization in the M versus H curve in PFM, PFT and PFW materials can be described on the basis of superexchange interaction at the B-site octahedral and also spin canting.

#### 4. Conclusions

Multiferroic PFT-PZT ceramics with a high percentage of perovskite phase were successfully synthesized by a solid-state reaction technique. XRD analysis showed a change in the crystal structure from cubic to mixed cubic/tetragonal with increasing PZT content. The Ti K-edge XANES spectra of all samples were very similar to those of Fe K-edge XANES spectra, indicating similar local structure around Fe and Ti ions. SEM observations reveal that the co-existence of two phases affects the sintering and grain growth behavior of the components. An analysis of dielectric constant with frequency was performed at various temperatures. Diffuse maxima and frequency dispersion were observed in the dielectric constant versus temperature plots. The samples exhibit a relaxor behavior around the

maximum dielectric constant characterized by a strongly diffused dielectric peak. There is significant change of dielectric properties between 1 kHz and other frequencies and occur a broad hump characteristic at 1 kHz. The materials exhibited square saturated magnetic hysteresis loops with 0.003 emu/g at room temperature. Saturated magnetization of all compositions showed no difference with increasing PZT content.

#### Acknowledgments

The authors would like to thank the Thailand Research Fund (TRF) and the Faculty of Science, Maejo University, for financial support. RY would like to acknowledge support from the NANOTEC-SUT Center of Excellence on Advanced Functional Nanomaterials.

#### References

- [1] Cheng, J., Yu, S., Chen, J., Meng, Z.: Appl. Phys. Lett. 89, 122911 (2006).
- [2] Kumar, A., Rivera, I., Katiyar, R.S., Scott, J.F.: Appl. Phys. Lett. 92, 132913 (2008).
- [3] Fang, B.-J., Ding, C.-L., Liu, W., Li, L.-Q., Tang, L.: Eur. Phys. J. Appl. Phys. 45, 20302 (2009).
- [4] Choudhary, R.N.P., Pradhan, D.K., Tirado, C.M., Bonilla, G.E., Katiyar, R.S.: J. Appl. Phys. 100, 084105 (2006).
- [5] Sharma, S., Singh, V., Kotnala, R.K., Ranjan, R., Dwivedi, R.K.: J. Alloys Compd. 614, 165–172 (2014).
- [6] Patil, D.R., Chougule, B.K.: J. Alloys Compd. 458, 335-339 (2008).

- [7] Ciomaga, C.E., Galassi, C., Prihor, F., Dumitru, I., Mitoseriu, L., Iordan, A.R., Airimioaei, M., Palamaru, M.N.: J. Alloys Compd. 485, 372–378 (2009).
- [8] Sanchez, D.A., Ortega, N., Kumar, A., Roque-Malherbe, R., Polanco, R., Scott, J.F., Katiyar, R.S.: AIP Adv. 1, 042169 (2011).
- [9] Falqui, A., Lampis, N., Geddo-Lehmann, A., Pinna, G.: J. Phys. Chem. B 109, 22967– 22970 (2005).
- [10] Choudhary, R.N.P., Rodriguez, C., Bhattacharya, P., Katiyar, R.S., Rinaldi, C.: J. Magn. Magn. Mater. 313, 253–260 (2007).
- [11] Lampis, N., Franchini, C., Satta, G., Geddo-Lehmann, A., Massidda, S.: Phys. Rev. B 69, 064412 (2004).
- [12] Zhang, X.Y., Zhao, X., Lai, C.W., Wang, J., Tang, X.G., Dai, J.Y.: Appl. Phys. Lett. 85, 4190–4192 (2004).
- [13] Xu, G., Weng, W.J., Yao, J.X., Du, P.Y., Han, G.R.: Microelectron. Eng. 66, 568–573 (2003).
- [14] Randall, C.A., Kim, N., Kucera, J.-P., Cao, W., Shrout, T.R.: J. Am. Ceram. Soc. 81, 677–688 (1998).
- [15] Swartz, S.L., Shrout, T.R., Schulze, W.A., Cross, L.E.: J. Am. Ceram. Soc. 67, 311–315 (1984).
- [16] Wongmaneerung, R., Jantaratana, P., Yimnirun, R., Ananta, S.: J. Supercond. Nov. Magn. 26, 371–379 (2013).

- [17] Wongmaneerung, R., Jantaratana, P., Yimnirun, R., Ananta, S.: Ceram. Intl. 40, 2299–2304 (2014).
- [18] Moulson, A.J., Herbert, J.M.: Electroceramics: Materials, Properties and Application.
  2<sup>nd</sup> ed. John Wiley & Sons, West Sussex (2003).
- [19] Abdelkefi, H., Khemakhem, H., Vélu, G., Carru, J.C., Mühll R.V.: J. Alloys Compd. 399, 1–6 (2005).
- [20] Zhu, W.Z., Yan, M., Mantas, P.Q., Baptista, J.L., Kholkin, A.L.: J. Mater. Res. 17, 1779–1784 (2002).
- [21] Nomura, S., Takabayashi, H., Nakagawa, T.: Jpn. J. Appl. Phys. 7, 600-604 (1968).
- [22] Zhu, W.Z., Yan, M., Kholkin, A.L., Mantas, P.Q., Baptista, J.L.: Mater. Chem. Phys. 82, 263–267 (2003).
- [23] Kulawik, J., Szwagierczak, D.: J. Eur. Ceram. Soc. 27, 2281-2286 (2007).
- [24] Kanamadi, C.M., Das, B.K., Kim, C.W., Kang, D.I., Cha, H.G., Ji, E.S., Jadhav, A.P., Jun, B.-E., Jeong, J.H., Choi, B.C., Chougule, B.K., Kang, Y.S.: Mater. Chem. Phys. 116, 6–10 (2009).
- [25] Zhao, Z., Zhao, V.Z., Buscaglia, V., Viviani, M., Buscaglia, M.T., Mitoseriu, L., Testino, A., Nygren, M., Johnsson, M., Nanni, P.: Phys. Rev. B 70, 024107 (2004).
- [26] Hoshina, T., Wada, S., Kuroiwa, Y., Tsurumi, T.: Appl. Phys. Lett., 93, 192914 (2008).
- [27] Wada, S., Kondo, S., Moriyoshi, C., Kuroiwa, Y.: Jpn. J. Appl. Phys., 47, 7612–7616 (2008).

- [28] Wada, S., Yasuno, H., Hoshina, T., Nam, S.M., Kakemoto, H., Tsurumi, T.: Jpn. J. Appl. Phys. Part 1: Regul. Pap. Short Notes Rev. Pap., 42, 6188–6195 (2003).
- [29] Peng, W., Lemée, N., Dellis, J.-L., Shvartsman, V.V., Borisov, P., Kleemann, W., Trontelj, Z., Holc, J., Kosec, M., Blinc, R., Karkut, M.G.: Appl. Phys. Lett. 95, 132507 (2009).
- [30] Sanchez, D.A., Kumar, A., Ortega, N., Katiyar, R.S., Scott, J.F.: Appl. Phys. Lett. 97, 202910 (2010).
- [31] Kumar, A., Katiyar, R.S., Rinaldi, C., Lushnikov, S.G., Shaplygina, T.A.: Appl. Phys. Lett. 93, 232902 (2008).
- [32] Rai, R., Kholkin, A.L., Sharma, S.: J. Alloys Compd. 506, 815-819 (2010).
- [33] Schmid, H.: Ferroelectrics 162, 317 (1994).
- [34] Galasso, F.S.: Perovskite and High T<sub>c</sub> Superconductors, Gordon and Breach, New York (1990).
- [35] Franchini, C.: private communication.
- [36] Blinc, R., Cevc, P., Zorko, A., Holc, J., Kosec, M., Trontelj, Z., Pirnat, J., Dalal, N., Ramachandran, V., Krzystek, J.: J. Appl. Phys. 101, 033901 (2007).

#### List of Table Captions

Table 1 Physical properties of (1-x)PFT-xPZT multiferroic ceramics sintered at 1200 °C.

Table 2 Dielectric properties of 0.7PFT-0.3PZT and 0.6PFT-0.4PZT multiferroic ceramics

#### **List of Figure Captions**

Fig. 1 XRD patterns of (1-x)PFT-xPZT multiferroic ceramics sintered at 1200 °C.

Fig. 2 Fe K-edge XANES spectra of (1-x)PFT-xPZT (x = 0.1, 0.3 and 0.5) multiferroic ceramics compared with the Fe K-edge XANES spectra of Fe metal, FeO, Fe<sub>2</sub>O<sub>3</sub> and Fe<sub>3</sub>O<sub>4</sub> standards.

Fig. 3 Fe K-edge XANES spectra of PFT-PZT samples compared with Ti K-edge of PZT single crystal.

Fig. 4 (a) Fe K-edge and (b) Ti K-edge XANES spectra of (1-x)PFT-xPZT (x = 0.1, 0.3 and 0.5).

Fig. 5 SEM micrographs of (1-x)PFT-xPZT multiferroic ceramics sintered at 1200 °C with (a) x = 0.1, (b) 0.2, (c) 0.3, (d) 0.4 and (e) 0.5

Fig. 6 Temperature dependence of the real part of the dielectric constant for (1-x)PFT-xPZT multiferroic ceramics with (a) x = 0.3 and (b) 0.4.

Fig. 7 M-H hysteresis loops of (1-x)PFT-xPZT multiferroic ceramics.

Table Click here to download Table: Table.doc

Table 1

Composition (x) (weight fraction)  0.1 0.2	Relative density	Grain size
	(%)	(μm)
	90	6.7-33.3
	92	
0.3	95	1.5-7.5
0.4	94	1.25-1.75
0.5	91	1.0-5.33

Table 2

Composition (x) (weight fraction)	Frequency (kHz)	T <sub>max</sub>	$\varepsilon_{\rm r}$ at $T_{\rm max}$
10	100	23988.35	
100	95	15615.07	
1000	75	5189.10	
0.4	1	145	77629.54
	10	140	17934.51
	100	130	12599.35
	1000	130	9670.00

Figure Click here to download Figure: figure.doc

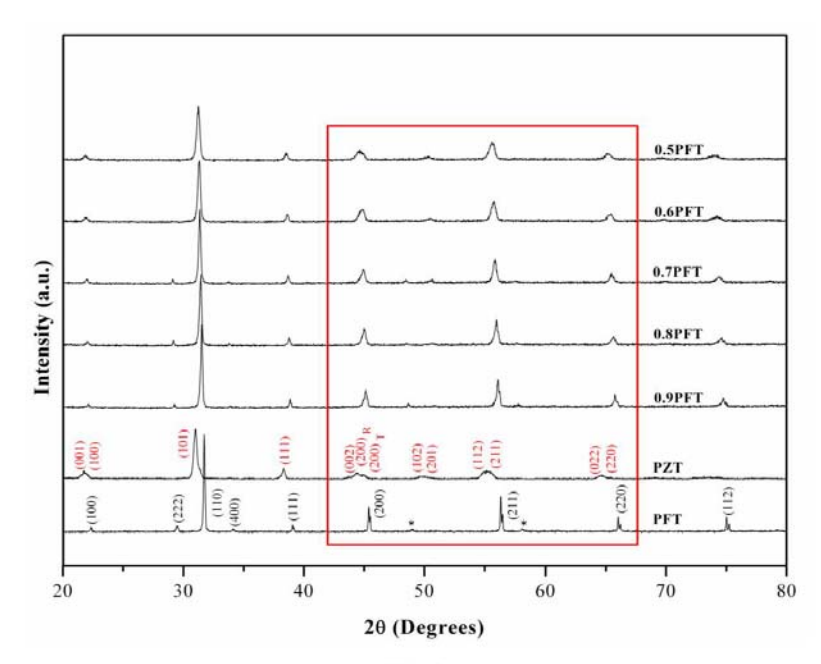


Fig. 1

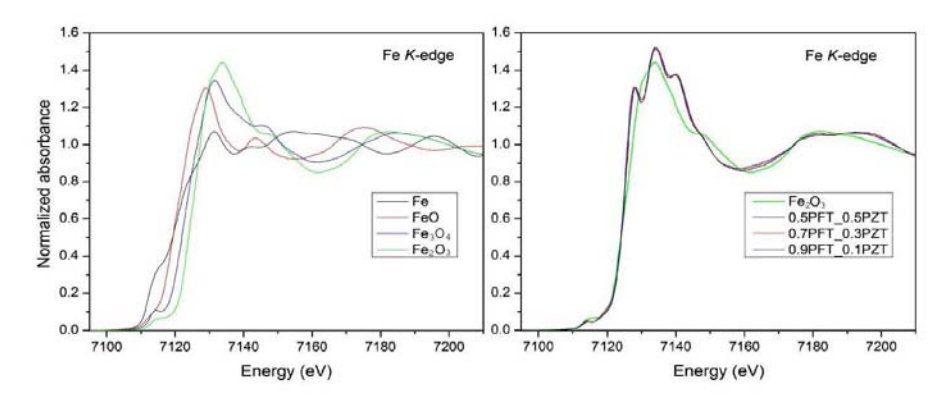


Fig. 2

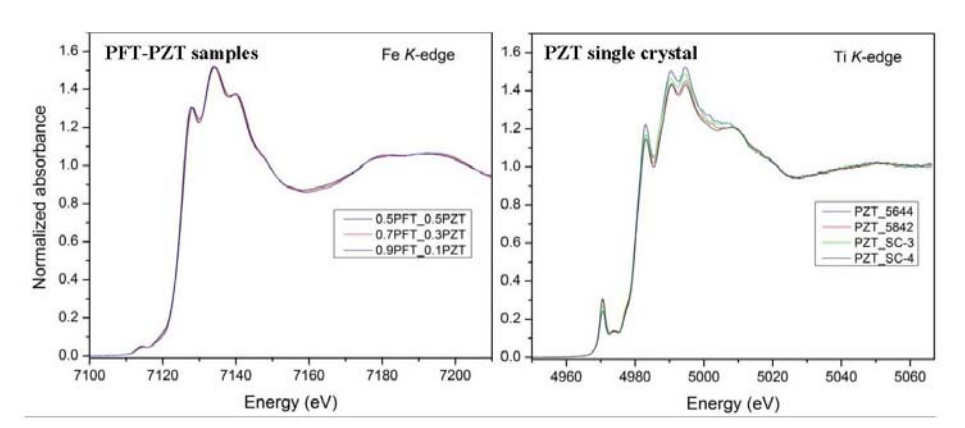


Fig. 3

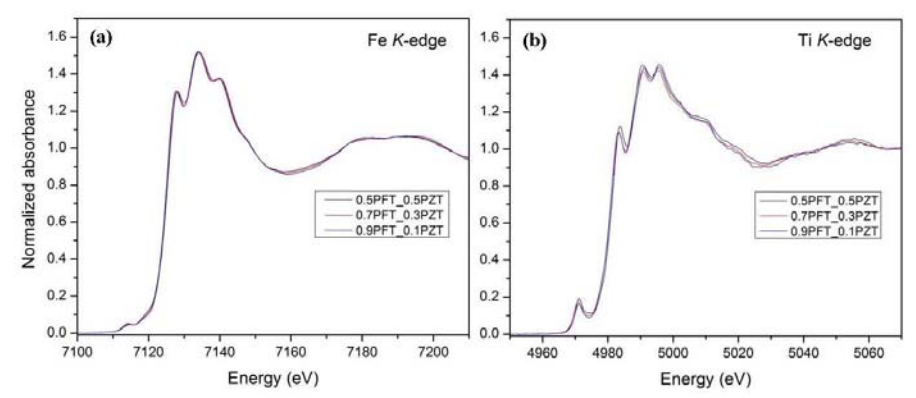


Fig. 4

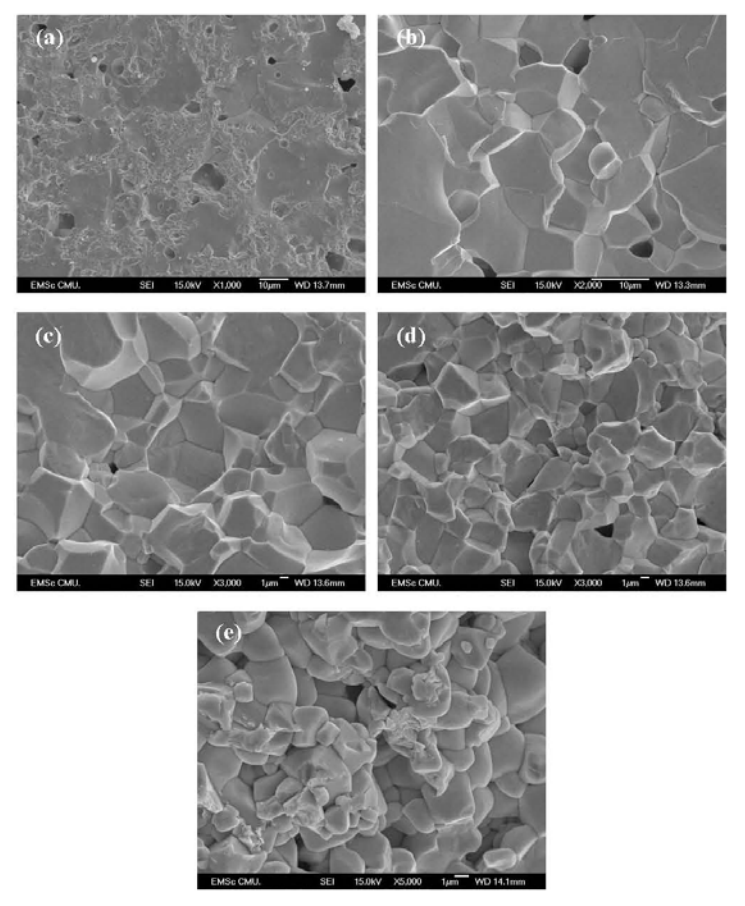
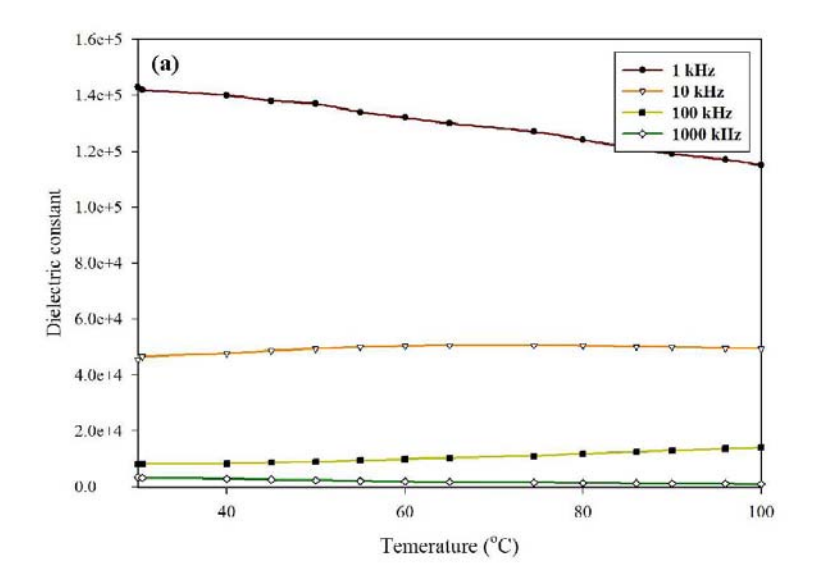


Fig. 5



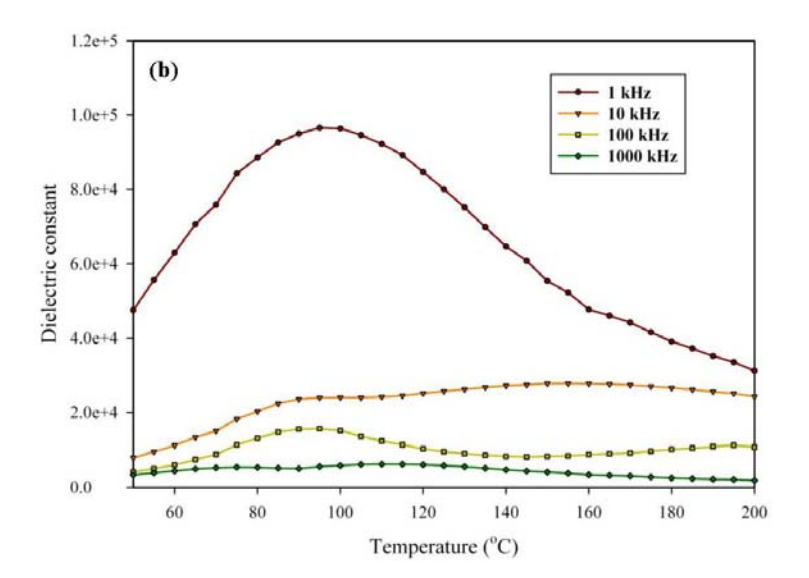


Fig. 6

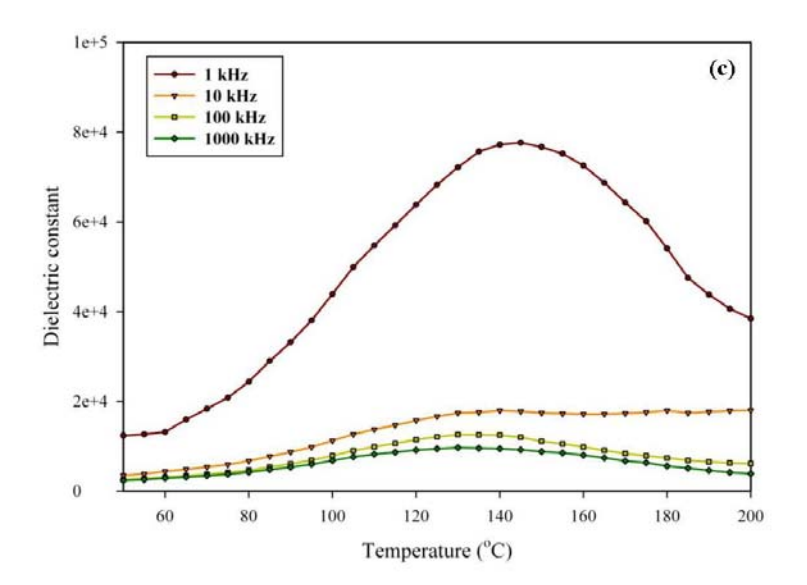


Fig. 6 (continue)

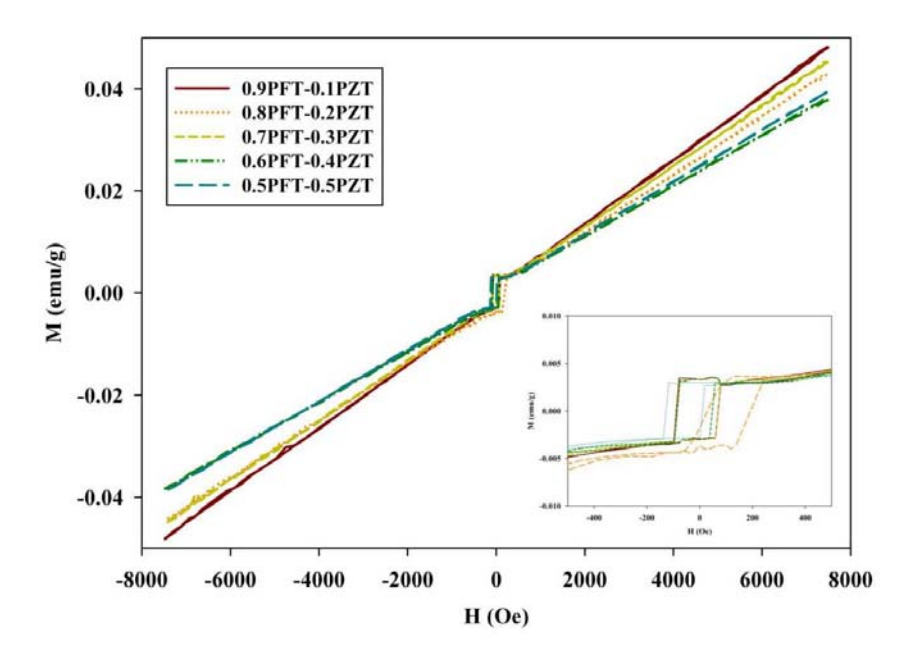
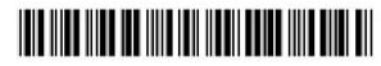


Fig. 7

# การเสนอผลงานทางวิชาการระดับชาติและนานาชาติ



STT39-0365





Science Society of Thailand Under the Royal Patronage of His Majesty the King, Faculty of Science, Chulalongkorn
University, Phya Thai Rd., Bangkok 10330
Tel: 0-2218-5245 Fax. 0-2252-4516
E-mail: stt39@scisoc.or.th

#### Acknowledgement

Dear Rewadee Wongmaneerung,

The secretariat committee of STT39 would like to inform you that we have received your STT39 registration information for ID: 0365 and e-mail address: re\_nok@yahoo.com

The secretariat committee of STT39 have received your registration as: Participant with paper submission

We recieved the payment as -

with amount 0.00 baht ( บาทถวน )

Your submitted paper entitiled -

was reviewed from academic subcommittee of STT with the result : No paper submission

Sincerely yours,

Associate Professor Dr. Thararat Supasiri



# STRUCTURE AND MAGNETIC PROPERTIES OF BISMUTH FERRITE-FERROELECTRIC-BASED COMPOSITES

Rewadee Wongmaneerung<sup>1,\*</sup>

<sup>1</sup>Materials Science Program, Faculty of Science, Maejo University, Chiang Mai 50290, Thailand

\*e-mail: re nok@yahoo.com

**Abstract:** Binary and ternary multiferroic composites (1-x)BF-xPT, (1-x)BF-xPMN and (1-x)BF-x(0.9PMN-0.1PT) were fabricated by a traditional ceramic process. The effect of ferroelectric contents on phase assemblage, microstructure and magnetic properties were examined by XRD, SEM and VSM, respectively. The results indicate that XRD spectra of BF-PT and BF-PMN systems show perovskite structure ferrite and ferroelectric with a considerable amount of Bi<sub>24</sub>(Bi<sub>1.04</sub>Fe<sub>0.84</sub>)O<sub>40</sub> phase. Besides BF-(0.9PMN-0.1PT) system, XRD patterns displayed mixed BF, PMN and PT phases. In addition, the presence of secondary phases (Bi<sub>2</sub>Fe<sub>4</sub>O<sub>9</sub> and Fe<sub>2</sub>O<sub>3</sub>) was observed. The magnetic properties are generally seen to reduce with an increase in the content of the ferroelectric phase. It should be mentioned that the *M-H* loops of BF-PT composites completely differs from those of BF-PMN and BF-(0.9PMN-0.1PT) composites at room temperature. They exhibit superparamagnetic behavior. On the other hand, BF-PMN and BF-(0.9PMN-0.1PT) composites exhibit weak ferromagnetism behavior, as shown in Figure 1.

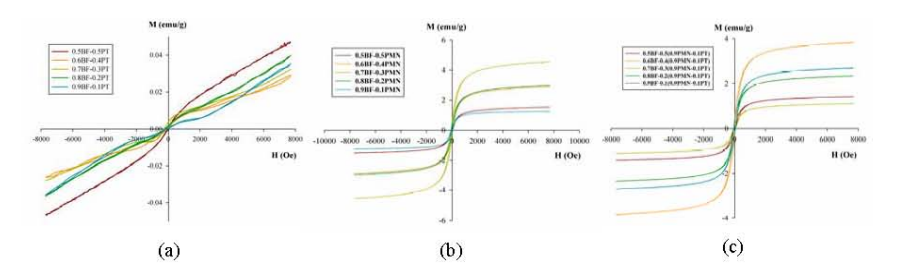


Figure 1 M–H hysteresis loops of (1-x)BF-xferroelectric composites sintered at 800 °C with (a) PT, (b) PMN and (c) 0.9PMN-0.1PT.

#### References:

- 1. Cohen RE, Nature 1992; 358: 136-138.
- Smolenskii GA, Isupov VA, Agranovskaya AI, Krainik NN, Sov. Phys. Solid State 1961; 2; 2651-2654.
- Mazumder R, Sujatha Devi P, Bhattacharya D, Choudhury P, Sen A, Raja M, Appl. Phys. Lett. 2007; 91: 062510-062513.

**Acknowledgements:** The authors would like to thank the Thailand Research Fund (TRF) and the Faculty of Science, Maejo University for financial support.

Keywords: multiferroic, composites, bismuth ferrite, ferroelectric, magnetic properties

#### SSP-039

### Synthesis and Characterization of Lead Iron Tantalate-Lead Zirconate Titanate Composites

Rewadee Wongmaneerung a.\*, Rattikorn Yimnirun and Supon Anantac

<sup>a</sup>Materials Science Program, Faculty of Science, Maejo University,
Chiang Mai 50290, Thailand

<sup>b</sup>School of Physics, Institute of Science, Suranaree University of Technology, and
NANOTEC-SUT Center of Excellence on Advanced Functional Nanomaterials,
Nakhon Ratchasima 30000, Thailand

<sup>c</sup>Department of Physics and Materials Science, Faculty of Science,
Chiang Mai University, Chiang Mai 50200, Thailand

The relaxor ferroelectric lead iron tantalate (Pb(Fe $_{0.5}$ Ta $_{0.5}$ )O $_3$ ) and normal ferroelectric lead zirconate titanate (PbZr $_{0.52}$ Ti $_{0.48}$ O $_3$ ) were prepared by mixing 50–90% Pb(Fe $_{0.5}$ Ta $_{0.5}$ )O $_3$  and 10–50% PbZr $_{0.52}$ Ti $_{0.48}$ O $_3$  with produces ceramic composites. Structural analysis of the synthesized powders and composites were performed by the X–ray diffraction data at room temperature. Microstructure and magnetic hysteresis were characterized by Scanning Electron Microscope (SEM) and Vibrating sample magnetometer (VSM) techniques, respectively. The results indicated that all powders and composites showed the perovskite structure and PbZr $_{0.52}$ Ti $_{0.48}$ O $_3$  phase was compatible with Pb(Fe $_{0.5}$ Ta $_{0.5}$ )O $_3$  phase. The SEM observations revealed that the coexisted two phases affect the sintering behavior. The composites exhibit weak magnetism because of super-paramagnetic cluster phenomenon.

Keywords: multiferroic, composites, lead iron tantalate, lead zirconate titanate, magnetic properties

\*Corresponding Author: R. Wonemaneerung, e-mail address: re\_nok@yahoo.com



International Congress on Natural Sciences and Engineering

## **Acceptance/Invitation Letter**

# International Congress on Natural Sciences and Engineering (ICNSE 2014)

May 7-9, 2014, Kyoto, Japan

Dear Rewade Wongmaneerung,

We are very pleased to inform you that your manuscript, "Structural, Dielectric and Magnetic Properties of Multiferroic (1-x)Pb(Ta0.5Fe0.5)O3-xPb(Zr0.53-Ti0.47)O3 Composites" (ICNSE-740) has been accepted for Poster presentation at the International Congress on Natural Sciences and Engineering (ICNSE 2014) in Kyoto, Japan. Decisions were made based on a double-blind review process. The exact time and room of your presentation session will be specified in the ICNSE Conference Program online at <a href="http://www.icnse.org/">http://www.icnse.org/</a> in the beginning of April, 2014.

Please make sure your manuscripts conform to the writing format which is available on the conference website. Manuscripts conform to the format guidelines are required to be included in the proceedings.

If you have any further questions, please do not hesitate to contact the secretariat of ICNSE 2014 by sending your email <a href="mailto:icnse@icnse.org">icnse@icnse.org</a> with your manuscript ID number listed above on all communications. Again, congratulations on the acceptance of your paper. On behalf of the Program Committee, we look forward to your full participation in the ICNSE 2014 Conference.

Yours Sincerely,
The Program Committee of ICNSE 2014



#### Structural, Dielectric and Magnetic Properties of Multiferroic

(1-x)Pb(Ta<sub>0.5</sub>Fe<sub>0.5</sub>)O<sub>3</sub>-xPb(Zr<sub>0.53</sub>-Ti<sub>0.47</sub>)O<sub>3</sub> Composites

R. Wongmaneerung\*

\*Faculty of Science, Maejo University, Chiang Mai 50290, Thailand

E-mail address: re\_nok@yahoo.com

#### Abstract

Multiferroic composites containing lead iron tantalate (PFT) and lead zirconate titanate (PZT) phases were fabricated by solid–state reaction, with 10–50 wt% of PZT. The present study combines X–ray diffraction, synchrotron X–rays absorption near edge, microstructure, dielectric and magnetic properties at room temperature. Composite samples based on mixed relaxor and normal ferroelectric powders were sintered at 1200 °C. The XRD data show no secondary phase over all compositions. The presence of PFT–PZT phases was also confirmed by the oxidation state and the local structure surrounding the Fe and Ti absorbing atoms, as observed in the Fe K and Ti K-edge XANES spectrum. The result demonstrates that the local structure of Fe and Ti ions have the same structure. Therefore, it could be concluded that the Ti ions are replaced by Fe ions. The microstructure of the sintered composites was dense with average grain size of 0.5–3 µm. High and broad maxima of dielectric permittivity reaching 80000 and 100000 at 1 kHz for 30 and 40 wt% of PZT concentration, respectively. Measurements of the magnetization of the investigated composites as a function of magnetic field exhibited square saturated magnetic hysteresis loops with 0.03 emu/g.

Keyword: Multiferroic; composite; lead iron tantalite; lead zirconate titanate

